J|A|C|S COMMUNICATIONS

Published on Web 10/19/2010

A Water-Soluble Xe@cryptophane-111 Complex Exhibits Very High Thermodynamic Stability and a Peculiar ^{129}Xe NMR Chemical Shift

Robert M. Fairchild,[†] Akil I. Joseph,[†] K. Travis Holman,*[,†] Heather A. Fogarty,[‡] Thierry Brotin,[‡] Jean-Pierre Dutasta,[‡] Céline Boutin,[§] Gaspard Huber,[§] and Patrick Berthault[§]

Department of Chemistry, Georgetown University, Washington, D.C. 20057, Laboratoire de Chimie, CNRS, Ecole Normale Supérieure de Lyon, 46 Allée D'Italie, F-69364, Lyon, France, and CEA, IRAMIS, Service Interdisciplinaire sur les Systèmes Moléculaires et les Matériaux, Laboratoire Structure et Dynamique par Résonance Magnétique, UMR CEA/CNRS 3299, 91191 Gif-sur-Yvette, France

Received August 11, 2010; E-mail: kth7@georgetown.edu

Abstract: The known xenon-binding (±)-cryptophane-111 (**1**) has been functionalized with six $[(\eta^5\text{-}C_5Me_5)Ru^{II}]^+$ ([Cp*Ru]$^+$) moieties to give, in 89% yield, the first water-soluble cryptophane-111 derivative, namely $[(Cp^*Ru)_6\mathbf{1}]Cl_6$ ([**2**]Cl_6). [**2**]Cl_6 exhibits a very high affinity for xenon in water, with a binding constant of 2.9(2) $\times$ 10^4 M^{-1} as measured by hyperpolarized ^{129}Xe NMR spectroscopy. The ^{129}Xe NMR chemical shift of the aqueous Xe@[**2**]$^{6+}$ species (308 ppm) resonates over 275 ppm downfield of the parent Xe@**1** species in $(CDCl_2)_2$ and greatly broadens the practical ^{129}Xe NMR chemical shift range made available by xenon-binding molecular hosts. Single crystal structures of [**2**][CF_3SO_3]$_6\cdot x$solvent and 0.75H_2O@**1**$\cdot$2$CHCl_3$ reveal the ability of the cryptophane-111 core to adapt its conformation to guests.

For two decades, xenon has received increasing attention as a potent tracer for MRI imaging and NMR-based sensing due to its enormous chemical shift range and the availability of laser-polarization techniques that enhance nuclear polarization, and thereby sensitivity, by several orders of magnitude.[1] A biosensing technology based upon transportation of the noble gas to biological targets via functionalized xenon-binding molecular hosts has been proposed[2] and is supported by several proof-of-concept experiments.[3,4] The conditions required for xenon-binding biosensors to be effective for possible *in vivo* applications are as follows: (i) a high xenon binding constant (K_a) in biological media; (ii) slow in−out exchange conditions on the ^{129}Xe NMR time scale, yet sufficient in−out exchange rates to allow optimization of sensitivity by renewal of the host cavity with hyperpolarized xenon; (iii) adequate longitudinal relaxation times of the bound xenon nucleus; and (iv) amenity to chemical functionalization.[4] Moreover, proposed multiplexing strategies[2,5] require several high affinity hosts whose xenon complexes resonate at significantly different ^{129}Xe NMR frequencies.

Some of us,[5−7] and others,[3,8] have already demonstrated that cryptophanes—most notably derivatives of (±)-cryptophane-**A** (Chart 1; R = OCH_3, $n = m = 2$)—are among[9] the best host candidates for ^{129}Xe NMR-based sensors. In 2007, the smallest cryptophane core synthesized to date, (±)-cryptophane-111 (**1**), was shown to exhibit the largest xenon binding constant ever measured in an organic solvent ($K_a \approx 1 \times 10^4$ M^{-1} at 293 K in 1,1,2,2-tetrachloroethane-d_2 (TCE-d_2)).[7] The exceptional binding constant is largely the consequence of an optimized size match between xenon ($V_{Xe} = 42$ Å^3) and the small, spheroidal, arene-lined cavity of the host ($V_c \leq 80$ Å^3), suggesting that water-soluble derivatives of **1** would be excellent candidates for ^{129}Xe NMR-based biosensors. Unlike the cryptophane-**A** core, however, the synthesis of water-soluble derivatives of **1** via the attachment of hydrophilic residues is limited by the lack of modifiable functional groups, though the recent halogen functionalization of **1** may represent important progress in this respect.[10] Herein we describe the first water-soluble derivative of **1**. η^6-Coordination of the arene rings by cationic, electron-withdrawing $[(\eta^5\text{-}C_5Me_5)Ru^{II}]^+$ moieties[11] (hereafter [Cp*Ru]$^+$) gives rise to the air stable chloride salt (±)-$[(Cp^*Ru)_6\mathbf{1}]Cl_6$, hereafter [**2**]$Cl_6$ (Chart 1). Unlike carboxylic acid derivatized cryptophanes, whose water solubility is attributed to the pH active acid groups, [**2**]Cl_6 is highly water-soluble at neutral pH (≥30 mM, 293 K). The xenon binding constant of [**2**]Cl_6 is arguably the highest ever reported for a molecular host, and the corresponding Xe@[**2**]$^{6+}$ complex displays a very high ^{129}Xe NMR frequency that portends value in multiplexed imaging/sensing applications.

Chart 1. General Cryptophane Structure (*e.g.* Cryptophane-111, **1**: R = H, $n = m = 1$; Cryptophane-**A**: R = OCH_3, $n = m = 2$) and Synthesis of the Permetalated, Water-Soluble Congener of **1**, [**2**]Cl_6[a]

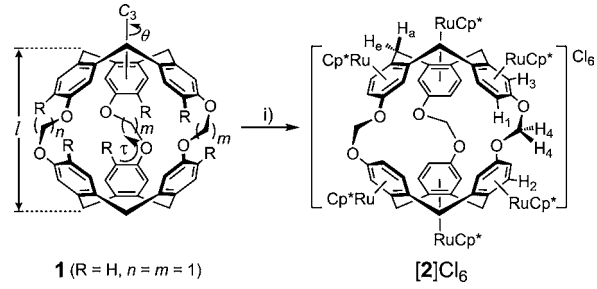

[a] (i) [Cp*Ru(μ_3-Cl)]$_4$, H_2O/THF, microwave, 89%.

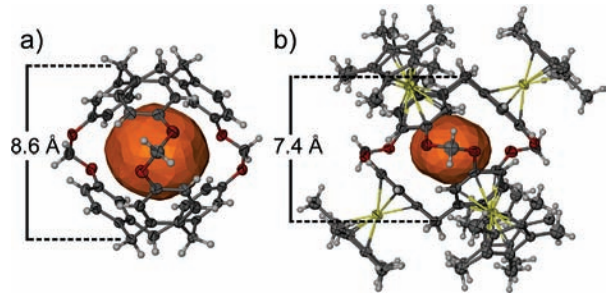

Figure 1. Thermal ellipsoid plots of (a) water-occupied **1** and (b) empty [**2**]$^{6+}$ from the X-ray crystal structures of 0.75H_2O@**1**$\cdot$2$CHCl_3$ and [**2**][CF_3SO_3]$_6\cdot x$$NO_2Me$, respectively. The host cavities are depicted in orange. Portions of disordered species are omitted.

[†] Georgetown University.
[‡] Ecole Normale Supérieure de Lyon.
[§] UMR CEA/CNRS 3299.

Consistent with the procedure reported for the permetalation of (±)-cryptophane-E,[11b] reaction of excess [Cp*Ru(μ_3-Cl)]$_4$ with **1** under microwave irradiation in anaerobic H_2O/THF gave [**2**]Cl_6 (89% yield), which was recrystallized to high purity from THF/H_2O. Unfortunately, single crystals of [**2**]Cl_6 grown from THF/H_2O proved problematic with respect to X-ray structure determination, but the single crystal structure of the triflate salt, [**2**][CF_3SO_3]$_6$·*x*solvent,[12] was successfully obtained and the [**2**]$^{6+}$ cation is depicted in Figure 1. Notably, in the absence of a suitably sized solvent guest (NO_2CH_3 and THF are too large for the cavity of [**2**]$^{6+}$), the host is found to be empty in the solid state, adopting a contracted conformation that minimizes the internal cavity volume. The empty conformation is characterized by a large twist angle of $\theta = 61(3)°$ between the two cyclotribenzylene (CTB) caps, as defined by the average dihedral angles between the arene ring centroids of OCH_2O-connected arenes with respect to the C_3 axis of the host (Chart 1; Figure S3). Twisting of the adjoined caps is facilitated by variations in the $C_{Ar}-C_{Ar}-O-CH_2$ dihedral angles, τ, as defined in Chart 1. These angles average $\tau = 177(2)°$ in the [**2**]$^{6+}$ cation, thereby effectively minimizing the length, *l*, of the host ($l = 7.4$ Å) and the cavity volume ($V_c = 32$ Å^3).

The observation of empty cryptophane [**2**]$^{6+}$ is unusual and is superficially at odds with the known host−guest properties of **1**.[7,13] Other cryptophanes are known to collapse upon emptying, via a partial inversion of one of the CTB caps.[14] The relative twisting of adjoined CTB caps, however, has recently been crystallographically identified as a mechanism by which an aryl bridged cryptophane can minimize its empty cavity volume or conform to various sized guests.[15] For the purposes of comparison with [**2**][CF_3SO_3]$_6$·*x*solvent, and to illustrate the conformational flexibility of the cryptophane-111 core, we also report here the single crystal structure of 0.75H_2O@**1**·2$CHCl_3$ (Figure 1).[16] Interestingly, when crystallized from $CHCl_3$, **1** scavenges a molecule of water—the only available guest that can fit within the host—from the solvent. Consequently, **1** adopts a more expanded, less twisted ($\theta = 18(1)°$) conformation such that the water-occupied cavity ($V_c = 69$ Å^3) exhibits approximately double the volume of the empty host cavity observed in [**2**][CF_3SO_3]$_6$·*x*solvent. This expanded conformation, which is likely similar to that adopted by **1** during xenon complexation, is achieved by minimizing the dihedral angles τ to 4(4)°, thereby maximizing the length of the host ($l = 8.6$ Å).

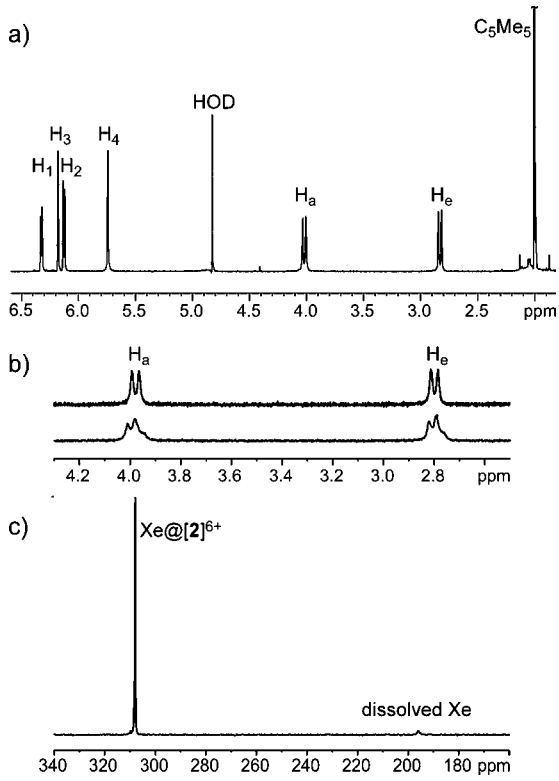

Figure 2. (a) ^{1}H NMR spectrum (500 MHz) of [**2**]Cl_6 in a degassed solution of D_2O at 293 K. (b) Partial ^{1}H NMR spectrum of [**2**]Cl_6 in degassed D_2O in the absence (top) and with 0.3 bar of xenon gas above the solution (bottom). Total host concentration: 1.7 mM. (c) Hyperpolarized ^{129}Xe NMR spectrum of [**2**]Cl_6 under the conditions described in part (b), bottom. The peak at 308 ppm is assigned to the Xe@[**2**]$^{6+}$ complex, and the tiny peak at 196 ppm is assigned to free, dissolved Xe.

The ^{1}H NMR spectrum of [**2**]Cl_6 in degassed D_2O (Figure 2a) gives the expected resonances, with coordination of the [Cp*Ru]$^+$ moieties inducing an upfield shift in most of the proton resonances as compared to **1**. At 293 K the ^{129}Xe NMR spectrum of [**2**]Cl_6 in D_2O and in the presence of Xe gas displays two signals, one at 196 ppm for free xenon in water and the other at 308 ppm assigned to the Xe@[**2**]$^{6+}$ complex (Figure 2c). Slow exchange conditions are encountered in both the ^{1}H and the ^{129}Xe NMR spectra of [**2**]Cl_6 (Figure 2b,c), allowing accurate determination of the binding constant without knowledge of the exact concentration of dissolved xenon, but with knowledge of the total host concentration. A xenon binding constant of $K_a = 2.9(2) \times 10^4$ M^{-1} ($\Delta G° = -6.0$ kcal·mol^{-1}) at 293 K has been extracted. This value is equal (within error) to the largest xenon binding constant ever reported for a molecular host, namely that reported for TAAC (Table 1)—a sparingly water-soluble triacetic acid derivative of cryptophane-**A**—in 20 mM aqueous phosphate buffer.[8] Curiously, TAAC exhibits a xenon binding constant that is nearly 5 times those determined by ^{129}Xe NMR for other water-soluble derivatives of cryptophane-**A**, including the structurally very similar, but notably less polar, hexaacetic acid derivative, **A-acid** (Table 1).[17]

It remains unclear whether metal functionalization formally increases or decreases the thermodynamic affinity of a cryptophane cavity for xenon. The near 3-fold greater xenon affinity of [**2**]Cl_6 in D_2O relative to **1** in TCE-d_2 is not unexpected and may largely be attributable to the hydrophobic effect. Indeed, the water-soluble congeners of other cryptophanes exhibit similarly larger aqueous xenon affinities relative to their organic-dissolved parents (Table 1). Further studies on different salts of [**2**]$^{6+}$, dissolved in organic solvents, will perhaps clarify this issue.

Table 1. Association Constants for Xenon Binding and ^{129}Xe Chemical Shifts of Known Xe@cryptophane Complexes

Cryptophane	R, *n*, *m*[a]	$K_a \times 10^{-3}$ M^{-1} [b]	solvent	δ_{Xe}[c]	ref
1	H, 1, 1	~10	TCE-d_2	31	7
[**2**]Cl_6	H, 1, 1	29(2)	D_2O	308	*d*
A (or **222**)	OCH_3, 2, 2	3.3[e]	TCE-d_2	63	6a
A-acid	OCH_2CO_2H, 2, 2	5.6−9.1	D_2O	64	5a
TAAC	OCH_3/OCH_2CO_2H, 2, 2	33(3)[f]	Aq. buffer	−	8
E (or **333**)	OCH_3, 3, 3	0.005−0.010[e]	TCE-d_2	30	21
E-acid	OCH_2CO_2H, 3, 3	0.6−2.9	D_2O	35	5a

[a] See Chart 1. [b] Determined by ^{129}Xe NMR spectroscopy at 293 K unless otherwise noted. [c] Xe@host species. [d] This work. [e] 278 K. [f] Determined by ITC and corroborated by fluorescence quenching.

The ^{129}Xe NMR chemical shift of xenon bound by cryptophanes has been the subject of study,[18] and the chemical shift of the Xe@[**2**]$^{6+}$ complex is one of the most remarkable features of this new complex. At 308 ppm, the aqueous Xe@[**2**]$^{6+}$ species resonates over 275 ppm downfield from the Xe@**1** species in TCE-d_2 (31 ppm). The enormous frequency difference—by far the largest observed for two xenon hosts possessing essentially the same internal cavity—is obviously not due to solvent effects. Table 1

gives the resonance frequencies of encapsulated xenon for some organic and water-soluble cryptophane congeneric pairs. The encapsulated xenon resonances of the organic-dissolved cryptophanes do not deviate more than a few ppm from the resonances of their water-dissolved congeners (e.g., Xe@**A**, 63 ppm vs Xe@**A**-**acid**, 64 ppm). In fact, all known Xe@cryptophane complexes resonate in the ^{129}Xe frequency range of ~30−80 ppm near room temperature. Thus, the six cationic, electron-withdrawing $[Cp^*Ru]^+$ moieties are predominantly responsible for the peculiar chemical shift of $[\mathbf{2}]^{6+}$, dramatically influencing the effect of the arene rings on the caged xenon. Exterior metal functionalization therefore greatly broadens the practical ^{129}Xe NMR chemical shift range made available by cryptophane hosts. This result suggests that it should be possible, using a single, optimized host skeleton (e.g., **1**), to design a family of hosts with comparable aqueous xenon affinities, but whose ^{129}Xe NMR frequency responses span nearly the entire known chemical shift range for a *naked* xenon atom (0−350 ppm). For example, it is hypothesized that xenon bound within the cavities of monometalated through pentametalated derivatives of **1**—more than a dozen new hosts, including regioisomers—will resonate with ^{129}Xe NMR frequencies that span the 31−308 ppm range defined by the nonmetalated Xe@**1** and hexametalated Xe@$\mathbf{2}^{6+}$ species. Moreover, cryptophane-**A** and its derivatives, which are also excellent hosts for xenon complexation, would be amenable to this approach. Indeed, metal functionalization, and functionalization with electron-withdrawing groups in general, may provide access to many hosts for multiplexed xenon sensing/imaging applications.[5]

As previously mentioned, an adequate xenon in−out exchange rate is mandatory for the ^{129}Xe NMR based biosensing approach. Obviously, it should be slow on the xenon chemical shift time scale in order to give rise to separate peaks for the caged and free xenon environments, but it should be fast enough to enable constant replenishment of the cage by hyperpolarized xenon. The presence of six $[Cp^*Ru]^+$ groups on the aromatic rings could conceivably slow down or even stop the in−out xenon exchange. This is not the case, as testified by 2D ^{129}Xe EXSY experiments (see Supporting Information). The extracted exchange rate constants are $k_{in} = 3.8 \times 10^5\ s^{-1}\ M^{-1}$ and $k_{out} = 13.1\ s^{-1}$ at 293 K. These values are consistent with the value of the binding constant considering that free cryptophane is present at 0.011 mM in solution under the 2D ^{129}Xe EXSY experimental conditions (1.05 bar of xenon).

In conclusion, we have demonstrated that the metalation of the six arene rings of cryptophane-111 by $[Cp^*Ru]^+$ moieties results in a cryptophane salt, $[\mathbf{2}]Cl_6$, that exhibits high water solubility over a wide pH range (including physiological pH) and a xenon affinity that matches the highest reported to date. The cationic, electron-withdrawing nature of the $[Cp^*Ru]^+$ moieties induces an enormous (>275 ppm) downfield chemical shift change for the caged xenon relative to the nonfunctionalized host. The exterior metalation approach constitutes a promising avenue toward a family of xenon-optimized biosensors for multiplexed imaging/sensing applications. Efforts along these lines and toward the further synthetic conjugation of such hosts—e.g. through the Cp* moieties[19]—are underway.

Acknowledgment. We are grateful for support from the U.S. National Science Foundation (DMR-0349316), the Ford Foundation (predoctoral fellowship for R.M.F.), Georgetown University (International Collaborative Research grant), and the French Ministry of Research (Projects ANR-06-PCVI-0023 BULPOXI and NT09-472096 GHOST). We thank Leonard J. Barbour for assisting with cavity volume calculations.[20]

Supporting Information Available: Experimental details for the syntheses, X-ray crystallography, and NMR experiments. This material is available free of charge via the Internet at http://pubs.acs.org.

References

(1) Cherubini, A.; Bifone, A. *Prog. NMR Spectrosc.* **2003**, *42*, 1–30.
(2) Spence, M. M.; Rubin, S. M.; Dimitrov, I. E.; Ruiz, E. J.; Wemmer, D. E.; Pines, A.; Qin Yao, S.; Tian, F.; Schultz, P. G. *Proc. Natl. Acad. Sci. U.S.A.* **2001**, *98*, 10654–10657.
(3) (a) Schröder, L.; Lowery, T. J.; Hilty, C.; Wemmer, D. E.; Pines, A. *Science* **2006**, *314*, 446–449. (b) Lowery, T. J.; Garcia, S.; Chavez, L.; Ruiz, E. J.; Wu, T.; Brotin, T.; Dutasta, J.-P.; King, D. S.; Schultz, P. G.; Pines, A.; Wemmer, D. E. *ChemBioChem* **2006**, *7*, 65–73. (c) Hilty, C.; Lowery, T. J.; Wemmer, D. E.; Pines, A. *Angew. Chem., Int. Ed.* **2006**, *45*, 70–73. (d) Wei, Q.; Seward, G. K.; Hill, P. A.; Patton, B.; Dimitrov, I. E.; Kuzma, N. N.; Dmochowski, I. J. *J. Am. Chem. Soc.* **2006**, *128*, 13274–13283. (e) Roy, V.; Brotin, T.; Dutasta, J.-P.; Charles, M.-H.; Delair, T.; Mallet, F.; Huber, G.; Desvaux, H.; Boulard, Y.; Berthault, P. *ChemPhysChem* **2007**, *8*, 2082–2085. (f) Schlundt, A.; Kilian, W.; Beyermann, M.; Sticht, J.; Günther, S.; Höpner, S.; Falk, K.; Roetzschke, O.; Mitschang, L.; Freund, C. *Angew. Chem., Int. Ed.* **2009**, *48*, 1–5. (f) Meldrum, T.; Seim, K. L.; Bajaj, V. J.; Palaniappan, K. K.; Wu, W.; Francis, M. B.; Wemmer, D. E.; Pines, A. *J. Am. Chem. Soc.* **2010**, *132*, 5936–5937.
(4) Berthault, P.; Huber, G.; Desvaux, H. *Prog. NMR Spectrosc.* **2009**, *55*, 35–60.
(5) (a) Huber, G.; Brotin, T.; Dubois, L.; Desvaux, H.; Dutasta, J.-P.; Berthault, P. *J. Am. Chem. Soc.* **2006**, *128*, 6239–6246. (b) Berthault, P.; Bogaert-Buchmann, A.; Desvaux, H.; Huber, G.; Boulard, Y. *J. Am. Chem. Soc.* **2008**, *130*, 16456–16457.
(6) (a) Bartik, K.; Luhmer, M.; Dutasta, J.-P.; Collet, A.; Reisse, J. *J. Am. Chem. Soc.* **1998**, *120*, 784–791. (b) Brotin, T.; Dutasta, J.-P. *Chem. Rev.* **2009**, *109*, 88–130.
(7) Fogarty, H. A.; Berthault, P.; Brotin, T.; Huber, G.; Desvaux, H.; Dutasta, J.-P. *J. Am. Chem. Soc.* **2007**, *129*, 10332–10333.
(8) Hill, P. A.; Wei, Q.; Troxler, T.; Dmochowski, I. J. *J. Am. Chem. Soc.* **2009**, *131*, 3069–3077.
(9) Other promising host candidates include the cucurbiturils and microporous nanoparticles. For example, see: (a) Kim, B. S.; Ko, Y. H.; Kim, Y.; Lee, H. J.; Selvapalam, N.; Lee, H. C.; Kim, K. *Chem. Commun.* **2008**, 2756–2758. (b) Miyahara, Y.; Abe, K.; Inazu, T. *Angew. Chem., Int. Ed.* **2002**, *41*, 3020–3023. (c) Lerouge, F.; Melnyk, O.; Durand, J.-O.; Raehm, L.; Berthault, P.; Huber, G.; Desvaux, H.; Constantinesco, A.; Choquet, P.; Detour, J.; Smaïhi, M. *J. Mater. Chem.* **2009**, *19*, 379–386.
(10) Traoré, T.; Delacour, L.; Garcia-Argote, S.; Berthault, P.; Cintrat, J.-C.; Rousseau, B. *Org. Lett.* **2010**, *12*, 960–962.
(11) (a) Fairchild, R. M.; Holman, K. T. *J. Am. Chem. Soc.* **2005**, *127*, 16364–16365. (b) Fairchild, R. M.; Holman, K. T. *Organometallics* **2007**, *26*, 3049–3053, 4086.
(12) Crystal data for $[\mathbf{2}][CF_3SO_3]_6 \cdot 1.5H_2O \cdot 9NO_2Me$, $C_{129}H_{158}F_{18}N_9O_{45}Ru_6S_6$, $M = 3695.42\ g \cdot mol^{-1}$, light brown prisms, 0.48 × 0.34 × 0.24 mm^3, monoclinic, space group *C*2/*m* (No. 12), $a = 25.8474(12)$ Å, $b = 18.9252(9)$ Å, $c = 17.7103(16)$ Å, $\beta = 125.01°$, $V = 7095.5(8)$ Å^3, $Z = 2$, $D_c = 1.730$ g/cm^3, $F_{000} = 3754$, Mo Kα radiation, $\lambda = 0.710\ 73$ Å, $T = 100(2)$ K, $2\theta_{max} = 54.0°$, 30 623 reflections collected, 7985 unique ($R_{int} = 0.0200$). Final GooF = 1.049, $R_1 = 0.0587$, $wR_2 = 0.1654$, *R* indices based on 6905 reflections with $I > 2\sigma(I)$ (refinement on F^2), 443 parameters, 86 restraints. Lp and absorption corrections applied, $\mu = 0.822\ mm^{-1}$.
(13) Chaffee, K. E.; Fogarty, H. A.; Brotin, T.; Goodson, B. M.; Dutasta, J.-P. *J. Phys. Chem. A* **2009**, *113*, 13675–13684.
(14) Mough, S. T.; Goeltz, J. C.; Holman, K. T. *Angew. Chem., Int. Ed.* **2004**, *43*, 5631–5635.
(15) Holman, K. T.; Drake, S. D.; Orr, G. W.; Steed, J. W.; Atwood, J. L. *Supramol. Chem.* **2010**, in press.
(16) Crystal data for $0.75H_2O@\mathbf{1} \cdot 2CHCl_3$, $C_{47}H_{39.5}Cl_6O_{6.75}$, $M = 924.99\ g \cdot mol^{-1}$, orthorhombic, *Pbcn* (No. 60), $a = 51.168(5)$ Å, $b = 10.0144(10)$ Å, $c = 25.099(3)$ Å, $V = 12861(2)$ Å^3, $Z = 12$, $D_c = 1.433$ g/cm^3, $F_{000} = 5730$, $2\theta_{max} = 50.0°$, 78 070 reflections collected, 11 310 unique ($R_{int} = 0.0607$). Final GooF = 1.037, $R_1 = 0.0462$, $wR_2 = 0.1074$, *R* indices based on 8407 reflections with $I > 2\sigma(I)$ (refinement on F^2), 867 parameters, 60 restraints. Lp and absorption corrections applied, $\mu = 0.453\ mm^{-1}$.
(17) A large discrepancy is often found between binding constants measured by NMR and by other methods, *e.g.* isothermal titration calorimetry. For instance, see: ref 8 and Sessler, J. L.; Gross, D. E.; Cho, W.-S.; Lynch, V. M.; Schmidtchen, F. P.; Bates, G. W.; Light, M. E.; Gale, P. A. *J. Am. Chem. Soc.* **2006**, *128*, 12281–12288. The present NMR measurement takes advantage of slow-exchange conditions in both the ^{129}Xe and ^{1}H NMR spectra and is very accurate. For further discussion on this point, see Supporting Information.
(18) (a) Sears, D. N.; Jameson, C. J. *J. Chem. Phys.* **2003**, *119*, 12231–12244. (b) Ruiz, E. J.; Sears, D. N.; Pines, A.; Jameson, C. J. *J. Am. Chem. Soc.* **2006**, *128*, 16980–16988.
(19) Fairchild, R. M.; Holman, K. T. *Organometallics* **2008**, *27*, 1823–1833.
(20) (a) Barbour, L. *J. Supramol. Chem.* **2001**, *1*, 189–191. (b) Connolly, M. L. *J. Mol. Graph.* **1993**, *11*, 139–141.
(21) Brotin, T.; Dutasta, J.-P. *Eur. J. Org. Chem.* **2003**, 973–984.

JA1071515